International Journal of Science and Research (IJSR)
ISSN: 2319-7064
Impact Factor 2024: 7.101

Utilization of Palladium-Doped MoS_2 Hybrid Structures for the Micro-Trace Detection of Arsenic (III) Ions

Namita[1], Naushad Alam[1], Jamilur R. Ansari[2]

[1]Department of Physics, Lalit Narayan Mithila University, Darbhanga-846004, Bihar, India
Email: *missnamita9[at]gmail.com*

[2]Department of Applied Science, LIET, Alwar-Tijara-Delhi, Highway, Chikani, Alwar 301028, Rajasthan, India

Corresponding Authors
Professor Naushad Alam, Email: *nalam8841[at]gmail.com*
Professor Jamilur R. Ansari, Email: *drjransari1[at]gmail.com*

Abstract: ***Molybdenum disulfide (MoS_2), a prominent two-dimensional transition metal dichalcogenide (TMD), is characterized by its remarkable mechanical properties, tunable bandgap, and layered structure, which offers a high surface area conducive for various catalytic and electronic applications. However, its relatively low electrical conductivity and limited active sites hinder its efficacy in electrochemical and catalytic processes. To address these shortcomings, palladium (Pd) nanoparticles (NPs) can be integrated into the MoS_2 matrix, resulting in a hybrid nanostructure that enhances charge transfer kinetics and catalytic performance. The synthesis of Pd-MoS_2 hybrid structure typically involves a two-step process: initial production of MoS_2 nanosheets via hydrothermal or liquid exfoliation methods, followed by the deposition of Pd nanoparticles through chemical reduction techniques. The development and characterization of Pd-MoS_2 hybrid structure have garnered significant research attention, driven by their superior physicochemical properties and extensive potential applications across catalysis, energy storage, and sensing domains. The synthesized Pd-MoS_2 hybrid structure exhibits improved electrical conductivity, enhanced catalytic efficiency, and an increased density of surface-active sites. These attributes render it particularly promising for electrocatalytic applications, such as the hydrogen evolution reaction (HER), fuel cells, supercapacitors, biosensors, and environmental remediation efforts. The synergistic interactions between Pd and MoS_2 nanosheets not only bolster the performance of the composite material but also pave the way for innovative design strategies tailored toward advanced materials with specific functionalities. Future research focused on optimizing synthesis parameters, achieving uniform nanoparticle dispersion, and ensuring long-term stability will be crucial for unlocking the comprehensive potential of the Pd-MoS_2 hybrid structure in next-generation technologies.***

Keywords: Nanocomposites, Electrochemical, Catalytic, hybrid structure, Sensing

1. Introduction

The integration of transition metal dichalcogenides (TMDs) with noble metal nanoparticles has opened new avenues for developing high-performance nanomaterials with enhanced catalytic[1], electrical [2], and optical properties[3]. Among these, molybdenum disulfide (MoS_2)-palladium (Pd) nanocomposites have emerged as promising hybrid materials due to their synergistic effects, which improve charge transfer, stability, and catalytic efficiency[4]. MoS_2, a layered 2D material with a structure similar to graphene, has attracted significant attention in various fields, including electrocatalysis[5], sensing [6], and energy storage[7], owing to its unique properties, such as a tunable bandgap, large surface area, and strong mechanical stability. However, despite its advantages, bulk MoS_2 suffers from low electrical conductivity and a limited number of active edge sites, which restricts its effectiveness in electrochemical applications. To overcome these limitations, palladium nanoparticles (Pd NPs) are incorporated into MoS_2 sheets, significantly enhancing its conductivity and catalytic activity [8]. Palladium, a highly conductive and catalytically active noble metal, has remarkable hydrogen adsorption properties, making it highly suitable for hydrogen evolution reactions (HER) [9], fuel cells[10], and CO oxidation processes[11]. By anchoring Pd nanoparticles onto exfoliated MoS_2 nanosheets, the hybrid nanocomposite benefits from increased active surface sites, improved electron mobility, and enhanced stability under operational conditions. MoS_2's bandgap gets reduced due to Pd's metallic nature, which enhances light absorption in photocatalytic and optoelectronic devices [12]. Pd nanoparticles act as active sites for catalytic reactions, enhancing MoS_2's efficiency in CO_2 reduction and organic pollutant degradation [13]. The composite material also exhibits improved mechanical strength and flexibility, which is beneficial for flexible electronics and wearable devices [14]. Furthermore, Pd nanoparticles enhance the thermal stability of MoS_2, making it more resistant to oxidation and high-temperature conditions. The Pd-MoS_2 system also demonstrates superior selectivity in catalytic applications, including hydrogenation and dehydrogenation reactions. In electrochemical applications, the hybrid material exhibits lower overpotential and faster charge transfer kinetics, making it suitable for fuel cells and supercapacitors[15].

The synthesis of MoS_2-Pd nanocomposites can be achieved through various methods, including hydrothermal synthesis, chemical reduction, electrostatic self-assembly, and solvothermal techniques, each offering control over the size, dispersion, and morphology of Pd nanoparticles on the MoS_2 surface. The controlled synthesis of these nanocomposites is crucial, as factors such as nanoparticle size, distribution, and

interface interaction between MoS_2 and Pd play a significant role in determining their overall performance. The incorporation of Pd nanoparticles into MoS_2 matrices has led to significant advancements in applications such as hydrogen evolution reactions (HER), electrocatalysis, lithium-ion batteries, supercapacitors [16], biosensors, and environmental remediation. The enhanced conductivity and catalytic efficiency of MoS_2-Pd nanocomposites make them highly effective for energy conversion and storage devices[17], where efficient charge transfer and chemical stability are essential. Moreover, their ability to function as highly sensitive electrochemical sensors enables the detection of biomolecules, toxic gases, and heavy metals with high selectivity and sensitivity. In addition to energy and sensing applications, MoS_2-Pd nanocomposites have demonstrated potential in photocatalysis and wastewater treatment, where their catalytic efficiency can be utilized for the degradation of organic pollutants[18]. Pd nanoparticles help in suppressing the recombination of electron-hole pairs, significantly improving the efficiency of photocatalysis. The incorporation of Pd nanoparticles also improves MoS_2's hydrophilicity, which is beneficial for applications involving aqueous environments, such as water splitting and pollutant degradation[19].

The synergistic interaction between Pd and MoS_2 enhances the surface area and active sites, leading to improved electrocatalytic and photocatalytic performance. Moreover, the Pd-MoS_2 hybrid exhibits enhanced stability and durability, reducing degradation over prolonged use. As the demand for sustainable and high-performance materials continues to grow, MoS_2-Pd nanocomposites hold immense potential for the upcoming generation of technologies. By optimizing synthesis techniques, improving nanoparticle dispersion, and exploring different metal-functionalized MoS_2 hybrids[20] researchers can further enhance the material's efficiency and expand its range of applications. The continuous advancements in this field will play a crucial role in developing eco-friendly energy solutions, high-performance catalysts, and smart sensing devices, paving the way for significant breakthroughs in nanotechnology and material science.

2. Materials

Palladium chloride ($PdCl_2$), Sodium borohydride ($NaBH_4$), polyvinylpyrrolidone (PVP) , Cetyltrimethylammonium bromide (CTAB), Ethanol, deionized water, Sodium Hypophosphite (NaH_2PO_2) (85 mM), N-methyl-2-pyrrolidone (NMP), MoS_2 powders, Glassy Carbon Rotating Disk Electrode (GC-RDE), Alumina slurry, isopropanol and Nafion (V/V/V = 4/1/0.05).

2.1 Synthesis of Pd NPs

The synthesis of palladium (Pd) nanoparticles was carried out using a simple chemical reduction method, where sodium borohydride ($NaBH_4$) acts as a reducing agent and polyvinylpyrrolidone (PVP) as a stabilizer. First, a palladium precursor solution was prepared by dissolving $PdCl_2$ in deionized water with stirring until completely dissolved. To this solution, PVP was added as a stabilizing agent to prevent nanoparticle aggregation. Then, a freshly prepared $NaBH_4$ solution was added dropwise under continuous stirring, leading to a color change from yellow to dark brown or black, indicating the formation of Pd nanoparticles [21]. The reaction mixture was stirred for 30–60 minutes to ensure complete reduction. The nanoparticles were then purified by centrifugation at 8000–10000 rpm and washed multiple times with ethanol and deionized water to remove residual impurities. Finally, the purified Pd nanoparticles were dried at 60°C in a vacuum oven or under ambient conditions[22].

2.2 Synthesis of MoS_2 sheets

MoS_2 nanosheets were synthesized using a modified protocol derived from established methodologies in the literature [23]. In a typical procedure, 0.1 g of bulk MoS_2 powder was dispersed in 20 mL of NMP (N-Methyl-2-pyrrolidone) solvent. The mixture was vigorously stirred and allowed to rest overnight to ensure complete dispersion. Subsequent to this, the dispersion underwent sonication using a Sonics VCX-750 ultrasonic processor equipped with a flat head tip, operating at 750 W with a 30% amplitude setting for 90 minutes. Following sonication, the resulting dispersion was centrifuged at 5000 RPM for 45 minutes to isolate the supernatant containing the MoS_2 nanosheets.

2.3 Synthesis of Pd-MoS_2 nanosheets

In a 25 mL beaker, we sequentially combined 6 mL of a MoS_2 nanosheet suspension, 8 mL of a 2M CTAB solution, 0.355 mL of a 1% aqueous $PdCl_2$ solution, and 2 mL of an aqueous NaH_2PO_2 solution. The resulting reaction mixture was subjected to high-intensity ultrasonic irradiation using a Sonics ultrasonic processor (plate number VCX-750, equipped with a flat head tip, 750 W at 30% amplitude, 20 kHz) in a water bath maintained at a temperature of 30 to 35 °C. This process was conducted for 20 minutes, with periodic water replacements to ensure temperature stability. Following sonication, the product was collected via centrifugation and extensively washed with deionized water and ethanol. The precipitate obtained was then dried under a vacuum at 60 °C for 10 to 12 hours, prior to further characterization and electrochemical analysis [23], [24].

2.4 Electrode Preparation

Before electrochemical measurements, the GC-RDE was polished with 0.3 µm and 0.05 µm alumina slurries and sonicated in ethanol and deionized water. Catalyst suspensions were prepared by mixing deionized water, isopropanol, and Nafion (V/V/V = 4/1/0.05) for a stable ink. For the Pt/C catalyst, the dispersion was sonicated for 30 minutes, and 10 µL was deposited onto the GC-RDE (0.2471 cm^2). For MoS_2-Pd composites (25% Pd by weight), the sample was diluted to 1 mg/mL, sonicated for 30 min, and 10 µL was applied. All measurements were done under identical conditions, and the electrode was left to dry in a fume hood for one hour before testing [25].

3. Results and Discussion

3.1 UV Vis Analysis of Pd-MoS_2 Hybrid Structure

The UV-Vis absorption spectrum of the Pd-MoS_2 shown in **Figure 1** reflects both the intrinsic optical properties of MoS_2 and the influence of Pd nanoparticles on its electronic transitions. It provides crucial information about the interaction strength between the two components, the extent of plasmonic enhancement, and the modifications in electronic transitions[26]. In the 200- 250 nm wavelength range, a broad absorption feature is observed, which is primarily attributed to the accumulation of Pd nanoparticles and their plasmonic effects. This region corresponds to the inter-band transitions of palladium, which typically exhibit absorption due to the collective oscillation of free electrons in nanosized Pd particles. The presence of Pd nanoparticles enhances light absorption in this range, leading to an overall increase in absorbance. A sharp peak at 270 nm is distinctly observed, which can be associated with the surface plasmon resonance (SPR) of Pd nanoparticles or charge-transfer interactions between Pd and MoS_2. This peak indicates strong optical coupling between Pd and the underlying MoS_2 layers, suggesting an efficient electronic interaction at the hybrid interface. Beyond 300 nm, the absorption gradually decreases, followed by additional features that may correspond to MoS_2's characteristic excitonic transitions. The presence of Pd in the hybrid system influences the overall absorbance profile, leading to enhanced optical absorption in the UV range. This modification is particularly relevant for applications in photocatalysis, optoelectronics[27], and sensing, where strong light-matter interactions play a crucial role.

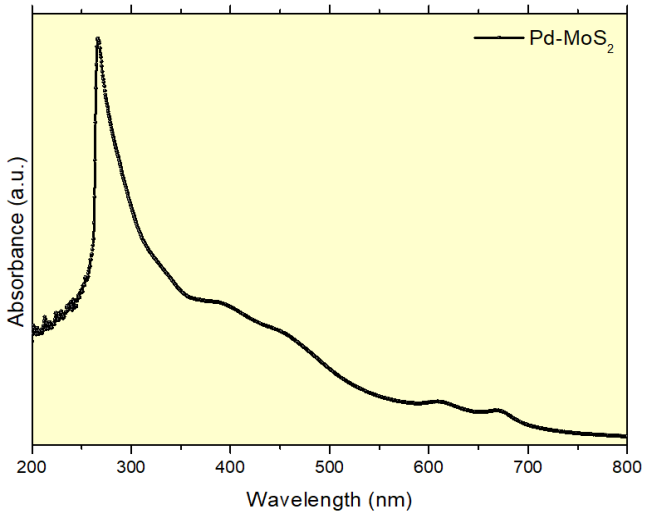

Figure 1: UV Vis spectra of Pd-MoS_2 hybrid structure

The UV-Vis spectral analysis thus confirms successful hybrid formation, with Pd nanoparticles contributing significantly to the optical response of the system. The small characteristic peaks of MoS_2, located at approximately 670 nm and 620 nm, arise due to spin-orbit splitting of the valence band at the K-point of the Brillouin zone. These peaks are crucial indicators of the material's semiconducting nature, with their intensity and position often influenced by structural modifications, doping or hybridization with metal nanoparticles. The incorporation of Pd introduces additional spectral features, primarily due to surface plasmon resonance (SPR) effects and charge transfer interactions.

A distinct plasmonic absorption band emerges in the 350–400 nm range, corresponding to the localized SPR of Pd nanoparticles. This peak is sensitive to particle size, shape, and interparticle spacing, with smaller nanoparticles exhibiting absorption closer to 350 nm, while larger or aggregated Pd structures can shift the peak toward longer wavelengths. The presence of Pd also alters the dielectric environment of MoS_2, affecting its band structure and excitonic transitions. This interaction often results in a slight redshift or broadening of the characteristic excitonic peaks, suggesting electronic coupling between Pd and MoS_2 layers. Additionally, the intensity of these peaks may decrease, indicating possible charge transfer from MoS_2 to Pd, which is beneficial for catalytic and sensing applications. The presence of palladium (Pd) nanoparticles in the MoS_2 matrix can lead to significant modifications in the absorption profile due to charge transfer interactions and plasmonic effects.

3.2 Photoluminescence analysis of Pd-MoS_2 Hybrid Structure

The photoluminescence (PL) spectrum (**Figure 2**) of the Pd-MoS_2 hybrid structure provides critical insights into its electronic structure, excitonic recombination, and charge transfer behavior. Pristine MoS_2, being a direct bandgap semiconductor in its monolayer form, exhibits strong PL emission primarily. However, in the presence of Pd nanoparticles, significant modifications in the PL spectrum occur due to charge transfer interactions, exciton quenching, and defect state formation. One of the most notable effects of Pd incorporation is the quenching of the MoS_2 excitonic peaks, which results from efficient electron transfer from the photoexcited MoS_2 to Pd. This occurs because Pd, being a metal, provides additional pathways for non-radiative recombination, thereby reducing the overall PL intensity. The extent of quenching depends on the dispersion, size, and interaction strength of Pd with MoS_2.

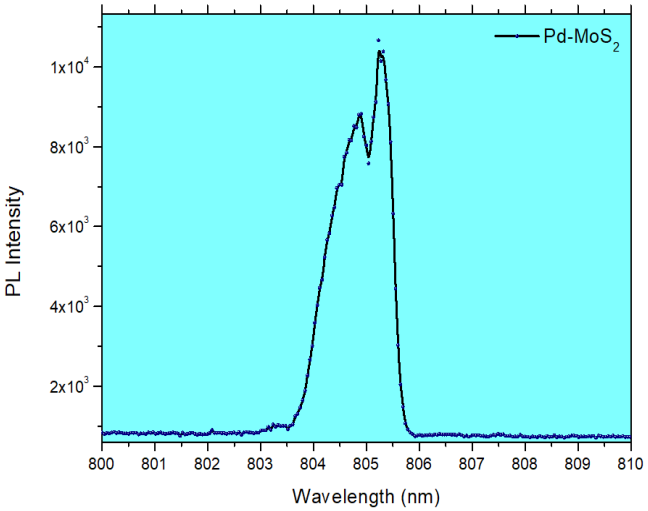

Figure 2: PL spectra of Pd-MoS_2 hybrid structure

The photoluminescence spectrum exhibits two distinct emission peaks: a sharp peak between 805–806 nm and another slightly lower-intensity peak between 804–805 nm, indicating strong radiative recombination processes within the hybrid system. The presence of these peaks suggests that Pd incorporation influences the optical properties of MoS_2, possibly through charge transfer effects or localized surface plasmon resonance (LSPR) of Pd nanoparticles [28]. The sharp nature of the 805–806 nm peak implies a well-defined

excitonic transition, which is associated with the modified band structure due to Pd-MoS_2 interactions. The peak at 804–805 nm further suggests a secondary electronic transition, possibly arising from defect states or localized energy levels introduced by Pd. The rest of the spectrum does not exhibit any additional prominent peaks at specific wavelengths, confirming that these two peaks dominate the PL response.

3.3 Raman Analysis of Pd-MoS_2 Hybrid Structure

The Raman spectrum of the Pd-MoS_2 hybrid structure provides valuable information about its vibrational modes, structural modifications, and the interaction between Pd nanoparticles and MoS_2. The intensity vs. Raman shift graph reveals several distinct peaks that indicate the presence of MoS_2 characteristic phonon modes along with additional features due to Pd incorporation (**Figure 3**). The spectrum exhibits significant modifications compared to pristine MoS_2, providing insight into vibrational modes, strain effects, and electronic interactions.

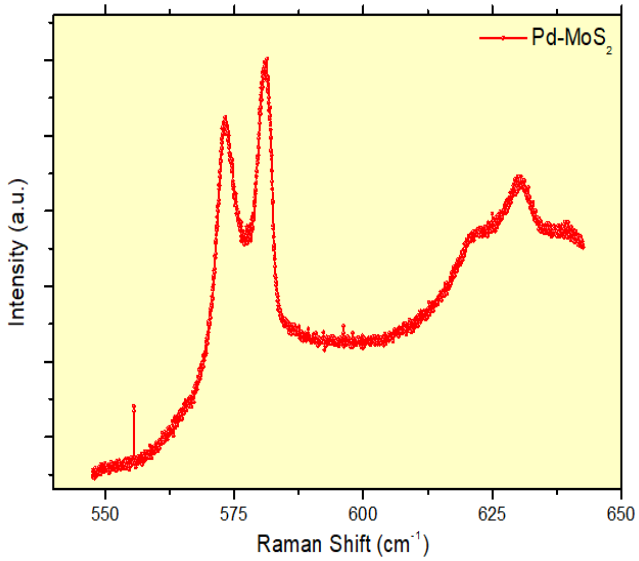

Figure 3: Raman spectra of Pd-MoS_2 hybrid structure

In pure MoS_2, two characteristic Raman-active modes are observed: the E^1_{2g} mode (~384 cm^{-1}), corresponding to the in-plane vibrations of Mo and S atoms, and the A_{1g} mode (~409 cm^{-1}), associated with the out-of-plane vibrations of sulphur atoms. The frequency difference ($\Delta\omega = A_{1g} - E^1_{2g}$) is around 25 cm^{-1} for monolayer MoS_2 and increases in multilayer structures due to interlayer coupling. Upon the incorporation of Pd nanoparticles, notable shifts in these Raman peaks occur due to charge transfer, strain, and defect formation. The E^1_{2g} mode often redshifts, indicating electron donation from Pd to MoS_2, which weakens Mo-S bonding. Conversely, the A_{1g} mode exhibits a blueshift, likely due to compressive strain induced by Pd interactions, altering the MoS_2 lattice dynamics. A sharp peak is observed around 570 cm^{-1}, which corresponds to defect-induced vibrational modes in MoS_2. This peak arises from Pd-induced strain in the MoS_2 lattice. Another sharp peak appears around 580 cm^{-1}, suggesting possible contributions from Pd-modulated vibrational modes. The presence of Pd nanoparticles can introduce charge transfer effects, which alter the phonon energies of MoS_2, leading to such peak shifts. Further, a strong peak is observed around 630 cm^{-1}, which may be linked to higher-order vibrational modes associated with Pd. This peak could also indicate Pd-S bonding interactions, suggesting that Pd atoms may be interacting with sulphur sites in MoS_2. Such interactions can influence the vibrational properties of the hybrid, leading to shifts or intensity variations in Raman-active modes.

3.4 TEM analysis of Pd-MoS_2 Hybrid Structure

The transmission electron microscopy (TEM) and high-resolution TEM (HRTEM) analysis of the Pd-MoS_2 hybrid structure provide detailed insights into the morphology, dispersion of Pd nanoparticles, and crystallinity of the hybrid material. **Figure 4(a)** captured at a 50 nm scale, reveals the overall structure of the Pd-MoS_2 hybrid, displaying thin MoS_2 nanosheets with uniformly dispersed Pd nanoparticles. The nanosheets appear slightly wrinkled, indicating their flexible nature, while Pd nanoparticles are distributed across the surface, suggesting strong interaction with the MoS_2 layers. The size and shape of Pd nanoparticles can be observed, with some agglomeration in certain regions.

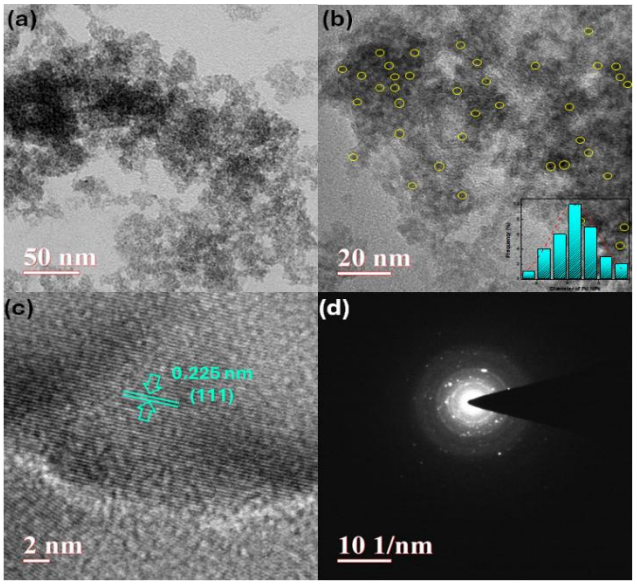

Figure 4: TEM analysis of (a,b) Pd-MoS_2 hybrid structure (c) HRTEM of Pd NPs and (d) SAED of Pd-MoS_2 hybrid structures

Figure 4(b) recorded at a 20 nm scale, provides a closer view of the Pd nanoparticle distribution on MoS_2. The image is accompanied by a graph representing the particle size distribution of the Pd nanoparticles. The histogram indicates that most nanoparticles are within a certain size range, but there is some variation in their diameters. A narrower distribution suggests well-controlled synthesis, whereas a broader distribution indicates size variation in the hybrid structure. The uniform dispersion of Pd nanoparticles suggests a successful hybridization process, and their size variations indicate controlled growth during synthesis. Some darker regions in the image may correspond to Pd-rich areas, reinforcing the idea of localized aggregation. At a much higher magnification, shown in **Figure 4(c),** taken at a 2 nm scale, highlights the crystalline nature of the hybrid, displaying well-resolved lattice fringes. The measured interplanar spacing of 0.225 nm corresponds to the (111) planes of pd nanoparticles in the MoS_2-Pd hybrid structure. confirming their structural integrity. The presence of clear

lattice fringes indicates high crystallinity, with minimal defects, and suggests strong interaction between Pd and MoS_2. The Pd nanoparticles appear as distinct bright spots on the MoS_2 lattice, further confirming their incorporation without significant lattice distortion. **Figure 4(d)** provides a broader field of view, showing the overall morphology of the hybrid material. This image emphasizes the sheet-like structure of MoS_2, with Pd nanoparticles appearing as small dark contrast spots. The larger-scale image suggests that the hybrid retains the layered structure of MoS_2 while effectively anchoring Pd nanoparticles, which is crucial for maintaining electronic and catalytic properties.

3.5 XPS Analysis of Pd-MoS_2 Hybrid Structure

X-ray Photoelectron Spectroscopy (XPS) provides a comprehensive understanding of its elemental composition, oxidation states, and chemical interactions. The XPS survey spectrum (**Figure 5a**) displays peaks corresponding to molybdenum (Mo), sulphur (S), palladium (Pd), carbon (C), and oxygen (O), confirming the presence of MoS_2 and Pd nanoparticles. The Mo 3d (~229 eV) and S 2p (~162 eV) peaks confirm the MoS_2 phase, while the Pd 3d (~337eV) peaks verify the successful integration of palladium. The absence of additional peaks related to other impurities suggests high purity of the synthesized Pd-MoS_2 hybrid. The Mo 3d spectrum (**Figure 5b**) provides deeper insights into the oxidation states of Mo in the hybrid. Two primary peaks at ~229 eV (Mo $3d_{5/2}$) and ~232 eV (Mo $3d_{3/2}$) confirm the presence of Mo^{4+}, which corresponds to MoS_2. A small shoulder peak at ~235–236 eV indicates the presence of Mo^{6+} species, which arise due to slight surface oxidation, leading to MoO_x formation [29]. The intensity of this oxidation peak is relatively low, confirming that MoS_2 remains largely intact with only minor oxidation effects. The Mo peaks in Pd-MoS_2 show a slight shift in binding energy compared to pristine MoS_2, which suggests strong electronic interactions between Pd and MoS_2, possibly due to charge transfer from MoS_2 to Pd.

In **Figure 5(c)**, the S 2p spectrum features a well-defined doublet corresponding to sulfide ions (S^{2-}). The S $2p_{3/2}$ peak at ~162 eV and the S $2p_{1/2}$ peak at ~163 eV are characteristic of MoS_2. These peaks remain sharp and intense, indicating that the sulfur atoms maintain their expected bonding environment. However, a slight shift in the binding energy compared to pure MoS_2 suggests an interaction between Pd and the sulfur sites in MoS_2. This shift is significant as it indicates charge redistribution at the Pd-MoS_2 interface, which may enhance catalytic or electronic properties. No significant peaks corresponding to oxidized sulfur species are detected, confirming that sulfur remains stable in the hybrid. The Pd 3d spectrum (**Figure 5d**) is crucial in determining the chemical state of palladium in the hybrid structure. Two major peaks are observed at ~337 eV (Pd $3d_{5/2}$) and ~343 eV (Pd $3d_{3/2}$), confirming the presence of metallic Pd^0. The well-defined nature of these peaks suggests that Pd is primarily in its elemental state, which is crucial for catalytic applications. The shift in Pd binding energy compared to pure Pd metal suggests strong coupling between Pd and MoS_2, leading to possible charge transfer effects that could influence the catalytic activity and electronic behaviour[30] of the hybrid.

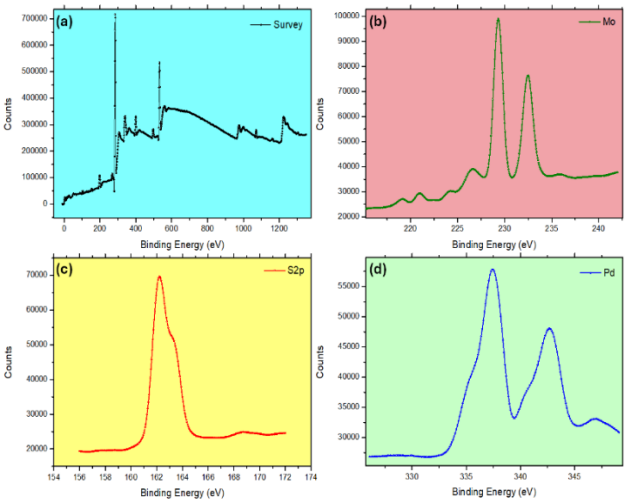

Figure 5: XPS analysis of Pd-MoS_2 hybrid structure (a) Survey, (b) Mo 3d, (c) S2p and (d) Pd 3d

3.6 Sensor performance of Arsenic analysis using DPV

The electrochemical sensing investigations of the Pd-MoS_2 hybrid structure were conducted using Differential Pulse Voltammetry (DPV), specifically tailored to detect Arsenic (As) in solution [29] . The DPV response of the Pd-MoS_2 hybrid was meticulously recorded at varying concentrations of As(III) ranging from 0.1 to 2.0 parts per billion (ppb), with a scan rate of 10 mV/s and within a potential window of 0.1 to 0.4 V. Observations revealed that the DPV response curves exhibited significant alterations in both shape and magnitude as the concentration of arsenic in the solution varied [31] . Notably, an increase in arsenic concentration was accompanied by a distinct shift in potential and a rise in the oxidation peak current, indicating the enhanced electrocatalytic properties of the modified electrode. Furthermore, the study was conducted at a pH of 6.0, which closely approximates physiological conditions, resulting in a comparatively lower oxidation peak. This underlines the relevance of the Pd-MoS_2 hybrid structure in potential applications for arsenic detection in biological systems.

The characteristics of the electrode curves reveal a distinctive trend, transitioning between cathodic and anodic peaks, ultimately exhibiting pseudocapacitive behavior as redox reactions take place at the electrodes. This behavior is linked to the reversible reactions between Pd ions at the electrodes and the surrounding solution interface. The Pd-MoS_2 hybrid structure, in particular, showcases a well-defined current wave, highlighting its electrochemical performance. A noteworthy observation is that the peak potential for this hybrid structure is registered at +0.26 V. As the concentration of As(III) is increased from 0.1 ppb to 2.0 ppb, there is a marked increase in the anodic peak current response. This enhancement can be attributed to the greater accessible surface area of the modified electrode, a factor that significantly boosts the electrocatalytic effect. The nanoscale dimensions of the material, combined with the presence of MoS_2, play a crucial role in facilitating electrocatalytic oxidation processes. Additionally, the Pd-MoS_2 hybrid structure exhibits a significantly larger differential pulse voltammetry (DPV) response area compared to pristine Pd nanoparticles (NPs). This observation signifies an enhanced capacity for charge storage[32], as indicated by the larger

DPV response peak of the Pd-MoS_2 hybrid compared to the unmodified NPs. Thus, it can be inferred that the MoS_2 coating substantially enhances the capacitance of the Pd NPs. At varying gravimetric concentrations of As(III), the discharge curves of the Pd-MoS_2 hybrid structure display a progressive shift in potential, as illustrated in the accompanying figure. According to prior research, the specific capacitance of the Pd-MoS_2 hybrid structure samples can be calculated using the following equation:

$$Cs = I\Delta t / m\Delta E$$

In this context, Cs, I, Δt, m, and ΔE represent specific capacitance, discharge current, discharge time, the active mass of the electrodes, and the IR discharge drops, respectively.

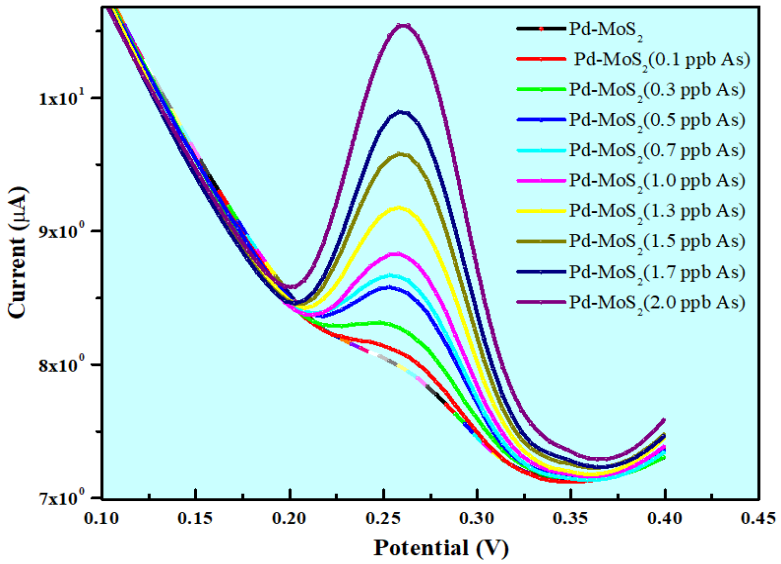

Figure 6: Differential Pulse Voltammetry (DPV) response of Pd-MoS_2 hybrid structure with varying Arsenic concentrations from 0.1–2.0 ppb

The findings reveal a notable trend: as current densities increase; the specific capacitance of the prepared electrodes tends to decrease. This behavior is indicative of pseudo capacitance, coupled with favorable electrochemical sensing characteristics. The reduction in specific capacitance can be attributed to the heightened current, which shortens the discharge time required for ions to penetrate the electrode structures. Furthermore, the data suggests that as current density rises, the discharge time diminishes, which consequently signifies an escalation in voltage drop across the electrodes. The specific capacitance of the electrodes modified with the Pd-MoS_2 hybrid structure has been calculated using the stipulated formula[33]. Remarkably, this hybrid configuration is shown to enhance specific capacitance by creating additional nucleation sites for energy storage, significantly benefiting overall performance. Incorporating palladium nanoparticles (Pd NPs) onto the MoS_2 sheets plays a pivotal role in improving electron transport both on the surface and within the Pd-MoS_2 hybrid structure. Collectively, these interactions not only elevate the electrodes' performance for electrochemical sensing but also contribute to a reduction in electrode resistance, enhancing their efficiency and responsiveness in practical applications.

4. Conclusion

The synthesis and characterization of MoS_2-Pd nanocomposites demonstrate a successful strategy to enhance the physicochemical properties of MoS_2 by incorporating highly active Pd nanoparticles. The characterization studies confirm the formation of a well-dispersed hybrid structure with improved surface area, stability, and conductivity. The synergistic interaction between MoS_2 and Pd nanoparticles enhances charge transfer processes and catalytic efficiency, making it a promising material for energy storage devices, fuel cells, and biosensors. The UV-Vis spectral response of the Pd-MoS_2 system provides valuable insights into the structural and optical properties, confirming successful hybridization and potential applications in optoelectronic and catalytic systems. The Raman analysis, therefore, provides strong evidence of Pd-MoS_2 interaction and highlights its potential for applications in catalysis, sensing, and electronic devices. The combination of TEM and HRTEM analysis confirms the successful integration of Pd into the MoS_2 matrix, demonstrating a well-dispersed and structurally coherent hybrid system suitable for potential applications in catalysis, sensing, and energy storage. The observed binding energy shifts in Mo, S, and Pd indicate strong electronic interactions between Pd and MoS_2 due to charge transfer from MoS_2 to Pd. This interaction is critical for improving catalytic efficiency as it can modulate the electronic structure of MoS_2 and enhance the activity of Pd sites. Additionally, the low presence of Mo^{6+} and Pd^{2+} species suggests that the hybrid material remains chemically stable, which is advantageous for applications in catalysis, sensing, and energy storage.

Credit authorship contribution agreement

Namita: Methodology, Investigation, Visualization, Writing - original draft, Writing - review & editing. **Naushad Alam** and **Jamilur R. Ansari:** Supervision, Validation, Project administration, funding acquisition. All the authors have read and discussed the data and agreed to the published version of the manuscript.

Acknowledgments

Namita and **Naushad Alam** gratefully acknowledge the support from LNMU in the form of a Research Fellowship. The authors thank Yonsei University for carrying out TEM/HRTEM characterizations. **Jamilur R. Ansari** is thankful to Yonsei University, South Korea, for the support under the BP Program.

References

[1] D. Deng, K.S. Novoselov, Q. Fu, N. Zheng, Z. Tian, X. Bao, Catalysis with two-dimensional materials and their heterostructures, Nat. Nanotechnol. 11 (2016) 218–230. https://doi.org/10.1038/nnano.2015.340.

[2] J.R. Ansari, M.F. Naseh, N. Singh, T. Sarkar, A. Datta, Unique photoluminescence response of MoS_2 quantum dots over a wide range of As (III) in aqueous media, Nanotechnology 32 (2021) 345708. https://doi.org/10.1088/1361-6528/abfee8.

[3] E. Kim, Y. Lee, C. Ko, Y. Park, J. Yeo, Y. Chen, H.S. Choe, F.I. Allen, J. Rho, S. Tongay, J. Wu, K. Kim, C.P. Grigoropoulos, Tuning the optical and electrical properties of MoS2 by selective Ag photo-reduction, Appl. Phys. Lett. 113 (2018) 013105. https://doi.org/10.1063/1.5022705.

[4] J.R. Ansari, N. Singh, S. Anwar, S. Mohapatra, A. Datta, Silver nanoparticles decorated two dimensional MoS2 nanosheets for enhanced photocatalytic activity, Colloids Surf. Physicochem. Eng. Asp. 635 (2022) 128102. https://doi.org/10.1016/j.colsurfa.2021.128102.

[5] J. Su, G. Li, X. Li, J. Chen, 2D/2D Heterojunctions for Catalysis, Adv. Sci. 6 (2019) 1801702. https://doi.org/10.1002/advs.201801702.

[6] M.F. Naseh, N. Singh, J.R. Ansari, A. Kumar, T. Sarkar, A. Datta, L-cysteine functionalized graphene quantum dots for sub-ppb detection of As (III), Nanotechnology 33 (2022) 065504. https://doi.org/10.1088/1361-6528/ac353b.

[7] Y. Li, J. Zhang, Q. Chen, X. Xia, M. Chen, Emerging of Heterostructure Materials in Energy Storage: A Review, Adv. Mater. 33 (2021) 2100855. https://doi.org/10.1002/adma.202100855.

[8] R. Quirós-Ovies, P. Bastante, S. Hettler, V. Vega-Mayoral, S. Aina, V. Balos, T. Pucher, A. Castellanos-Gomez, R. Arenal, J. Cabanillas-Gonzalez, E.M. Pérez, J. Santamaría, V. Sebastian, Chemically-Linked Heterostructures of Palladium Nanosheets and 2H-MoS_2, Small (2024) 2406030. https://doi.org/10.1002/smll.202406030.

[9] U. Aftab, M.Y. Solangi, A. Tahira, A. Hanan, M.I. Abro, A. Karsy, E. Dawi, M.A. Bhatti, R.H. Alshammari, A. Nafady, A. Gradone, R. Mazzaro, V. Morandi, A. Infantes-Molina, Z.H. Ibupoto, An advanced PdNPs@MoS_2 nanocomposite for efficient oxygen evolution reaction in alkaline media, RSC Adv. 13 (2023) 32413–32423. https://doi.org/10.1039/D3RA04738E.

[10] E. Antolini, Palladium in fuel cell catalysis, Energy Environ. Sci. 2 (2009) 915. https://doi.org/10.1039/b820837a.

[11] J. Wu, D. Chen, J. Chen, H. Wang, Structural and Composition Evolution of Palladium Catalyst for CO Oxidation under Steady-State Reaction Conditions, J. Phys. Chem. C 127 (2023) 6262–6270. https://doi.org/10.1021/acs.jpcc.2c07877.

[12] A. Wu, J. Li, B. Liu, W. Yang, Y. Jiang, L. Liu, X. Zhang, C. Xiong, X. Jiang, Band-gap tailoring and visible-light-driven photocatalytic performance of porous $(GaN)_{1-x}$ $(ZnO)_x$ solid solution, Dalton Trans. 46 (2017) 2643–2652. https://doi.org/10.1039/C6DT04428J.

[13] Namita, A. Khan, Arti, N. Alam, K.K. Sadasivuni, J.R. Ansari, MoS2 quantum dots and their diverse sensing applications, Emergent Mater. (2024). https://doi.org/10.1007/s42247-024-00656-7.

[14] Y. Wu, Y. Ma, H. Zheng, S. Ramakrishna, Piezoelectric materials for flexible and wearable electronics: A review, Mater. Des. 211 (2021) 110164. https://doi.org/10.1016/j.matdes.2021.110164.

[15] S. Sharma, P. Chand, Supercapacitor and electrochemical techniques: A brief review, Results Chem. 5 (2023) 100885. https://doi.org/10.1016/j.rechem.2023.100885.

[16] I.T. Bello, D. Tsotetsi, B. Shaku, O. Adedokun, D. Chen, M.S. Dhlamini, Advances in MoS2-based nanomaterials for supercapacitors, batteries and photovoltaics applications, J. Energy Storage 103 (2024) 114355. https://doi.org/10.1016/j.est.2024.114355.

[17] P. Das, Q. Fu, X. Bao, Z.-S. Wu, Recent advances in the preparation, characterization, and applications of two-dimensional heterostructures for energy storage and conversion, J. Mater. Chem. A 6 (2018) 21747–21784. https://doi.org/10.1039/C8TA04618B.

[18] Y. Shi, X.-K. Huang, Y. Wang, Y. Zhou, D.-R. Yang, F.-B. Wang, W. Gao, X.-H. Xia, Electronic Metal–Support Interaction To Modulate MoS_2 -Supported Pd Nanoparticles for the Degradation of Organic Dyes, ACS Appl. Nano Mater. 2 (2019) 3385–3393. https://doi.org/10.1021/acsanm.9b00297.

[19] M. Alaqarbeh, S.F. Adil, T. Ghrear, M. Khan, M. Bouachrine, A. Al-Warthan, Recent Progress in the Application of Palladium Nanoparticles: A Review, Catalysts 13 (2023) 1343. https://doi.org/10.3390/catal13101343.

[20] N. Mphuthi, L. Sikhwivhilu, S.S. Ray, Functionalization of 2D MoS2 Nanosheets with Various Metal and Metal Oxide Nanostructures: Their Properties and Application in Electrochemical Sensors, Biosensors 12 (2022) 386. https://doi.org/10.3390/bios12060386.

[21] A. Chen, C. Ostrom, Palladium-Based Nanomaterials: Synthesis and Electrochemical Applications, Chem. Rev. 115 (2015) 11999–12044. https://doi.org/10.1021/acs.chemrev.5b00324.

[22] M.V. Bravo, O.F. Silva, C. Adam, A.M. Granados, A simple way to prepare palladium nanoparticles decorated with cyclodextrins and ionic liquid. The effects of coating on the catalytic activity and colloidal stability, J. Mol. Liq. 304 (2020) 112725. https://doi.org/10.1016/j.molliq.2020.112725.

[23] G. H., V. S., N. Y. S., H. Devendrappa, A CTAB-assisted PANI-MoS_2 nanosheet flower morphology for the highly sensitive electrochemical detection of hydrazine, RSC Adv. 13 (2023) 34891–34903. https://doi.org/10.1039/D3RA06003A.

[24] B.B. Li, S.Z. Qiao, X.R. Zheng, X.J. Yang, Z.D. Cui, S.L. Zhu, Z.Y. Li, Y.Q. Liang, Pd coated MoS 2

nanoflowers for highly efficient hydrogen evolution reaction under irradiation, J. Power Sources 284 (2015) 68–76. https://doi.org/10.1016/j.jpowsour.2015.03.021.
[25] M. Pavličková, L. Lorencová, M. Hatala, M. Kováč, J. Tkáč, P. Gemeiner, Facile fabrication of screen-printed MoS2 electrodes for electrochemical sensing of dopamine, Sci. Rep. 12 (2022) 11900. https://doi.org/10.1038/s41598-022-16187-2.
[26] R. Ribeiro-Palau, C. Zhang, K. Watanabe, T. Taniguchi, J. Hone, C.R. Dean, Twistable electronics with dynamically rotatable heterostructures, Science 361 (2018) 690–693. https://doi.org/10.1126/science.aat6981.
[27] P.V. Pham, S.C. Bodepudi, K. Shehzad, Y. Liu, Y. Xu, B. Yu, X. Duan, 2D Heterostructures for Ubiquitous Electronics and Optoelectronics: Principles, Opportunities, and Challenges, Chem. Rev. 122 (2022) 6514–6613. https://doi.org/10.1021/acs.chemrev.1c00735.
[28] S. Marhaba, N. El Kawni, LOCALIZED SURFACE PLASMON RESONANCE OF PALLADIUM PARALLELEPIPED NANOPARTICLES, BAU J. - Sci. Technol. 4 (2023). https://doi.org/10.54729/2959-331X.1093.
[29] Madhavi, M. Kumar, J.R. Ansari, V. Kumar, S. Nagar, A. Sharma, Fe3O4 Coated SiO2 Magnetic Nanoparticles for Enhanced Antibacterial Activity and Electrochemical Sensing, Metals 12 (2022) 2145. https://doi.org/10.3390/met12122145.
[30] X. Li, H. Zhu, Two-dimensional MoS2: Properties, preparation, and applications, J. Materiomics 1 (2015) 33–44. https://doi.org/10.1016/j.jmat.2015.03.003.
[31] S. Agrahari, A.K. Singh, I. Tiwari, S. Srikrishna, Electrochemical deposition of Pd on MoS2 supported graphene nanoflakes over functionalised MWCNTs as an immunosensor for detection of lung cancer biomarker, Microchem. J. 196 (2024) 109698. https://doi.org/10.1016/j.microc.2023.109698.
[32] P. Das, Z.-S. Wu, F. Li, J. Liang, H.-M. Cheng, Two-dimensional energy materials: Opportunities and perspectives, Energy Storage Mater. 22 (2019) 15–17. https://doi.org/10.1016/j.ensm.2019.03.014.
[33] Y. Lan, L. Changshi, Reliably and accurately estimate energy in super-capacitor via a model of cyclic voltammetry, J. Energy Storage 75 (2024) 109688. https://doi.org/10.1016/j.est.2023.109688.